

## Preparation of bismuth oxide/titania composite particles and their photocatalytic activity to degradation of 4-chlorophenol

XU Jing-jing<sup>1,2</sup>, CHEN Min-dong<sup>1</sup>, FU De-gang<sup>3</sup>

1. Jiangsu Key Laboratory of Atmospheric Environment Monitoring and Pollution Control, College of Environmental Science and Engineering, Nanjing University of Information Science and Technology, Nanjing 210044, China;
2. State Key Laboratory of Hydrology-Water Resources and Hydraulic Engineering, Hohai University, Nanjing 210098, China
3. State Key Laboratory of Bioelectronics, Southeast University, Nanjing 210096, China

Received 22 October 2009; accepted 27 May 2010

**Abstract:** Bismuth oxide/titania, one interfacial composite semiconductor with high photocatalytic activity under solar light, was prepared at low temperature. The structure was characterized by X-ray diffractometry (XRD), scanning electron microscopy (SEM), brunauer-emmett-teller (BET), X-ray photoelectron spectroscopy (XPS) and diffuse reflection spectra (DRS). The results indicate that deposited titania nanoparticles on bismuth oxide surface have micro-nano structure, and this composite material exhibits porosity and increased surface hydroxyl groups. Furthermore, the as-prepared photocatalyst shows higher photocatalytic activity to the degradation of 4-chlorophenol than pure titania or P25 under sunlight.

**Key words:** bismuth oxide; titania; photocatalysis; 4-chlorophenol

### 1 Introduction

As a promising material, titania ( $\text{TiO}_2$ ) has been widely used in the photocatalytic degradation of polluted water and air[1–3]. However, the fast recombination rate of photo-generated charge carriers hinders the commercialization of this technology[1]. The energy gap between the valence band (VB) and conduction band (CB) in pure  $\text{TiO}_2$  is 3.2eV, so UV light is necessary to excite electrons on the  $\text{TiO}_2$  surface. To activate the photocatalysts with higher efficiency and longer wavelength, a number of strategies have been adopted. One of those strategies is to couple  $\text{TiO}_2$  with other semiconductor with appropriate CB and VB gaps. Photocatalysts  $\text{SiO}_2\text{-TiO}_2$ [4],  $\text{CdS-TiO}_2$ [5],  $\text{ZnO-TiO}_2$ [6] and  $\text{SnO}_2\text{-TiO}_2$ [7] have been prepared and used for many reactions.

It is well known that the lifetime of photo-induced charge carries is a key factor for improving photocatalytic activity, and using appropriate composite  $\text{TiO}_2$  can accelerate the separation of electrons and holes.

As for  $\text{ZnO-TiO}_2$ [8], the electrons transfer from the CB of  $\text{ZnO}$  to that of  $\text{TiO}_2$  under illumination, and conversely, the holes transfer from the VB of  $\text{TiO}_2$  to that of  $\text{ZnO}$ . Thus, the lifetime of photo-induced pairs increased since their recombination rate decreased. In order to extend the range of excitation energies of  $\text{TiO}_2$  into visible region, materials of narrow band gap were coupled with  $\text{TiO}_2$ . SHINGUU et al[9] reported that incorporated  $\text{WO}_3$  with  $\text{TiO}_2$  layers could modify the grain size and surface, and more important, it showed enhanced photocatalytic activity under visible light irradiation.

Bismuth oxide ( $\text{Bi}_2\text{O}_3$ ) is used in a variety of areas, such as sensor technology, optical coatings and electrochromic materials[10–12], due to its high refractive index, dielectric permittivity, marked photoconductivity and photoluminescence[10]. These special features explain the great effort devoted to the investigation of  $\text{Bi}_2\text{O}_3$  polymorphs over the past few years.  $\text{Bi}_2\text{O}_3$  has five main polymorphic forms, denoted by  $\alpha$ -,  $\beta$ -,  $\gamma$ -,  $\delta$ - and  $\omega$ - $\text{Bi}_2\text{O}_3$ [13–14]. Among them, the band gaps of the low-temperature  $\alpha$ -phase and high-

**Foundation item:** Project supported by the Scientific Research Foundation of Nanjing University of Information Science and Technology, China; Project (2010490511) supported by the Open Foundation of State Key Laboratory of Hydrology-Water Resources and Hydraulic Engineering, China

**Corresponding author:** XU Jing-jing, Tel: 86-25-58731090; E-mail: [xujj@seu.edu.cn](mailto:xujj@seu.edu.cn); [xujj@nuist.edu.cn](mailto:xujj@nuist.edu.cn)  
DOI: 10.1016/S1003-6326(11)60719-X

temperature metastable  $\beta$ -phase are 2.85 eV and 2.58 eV, respectively[15]. Thus, Bi/TiO<sub>2</sub> may exhibit excellent photocatalytic activity. KANG et al[16] found that without H<sub>2</sub>O addition, Bi/TiO<sub>2</sub> exhibited higher photocatalytic activity than TiO<sub>2</sub> in decomposing CH<sub>3</sub>CHO. However, HONG et al[17] reported that whether adding H<sub>2</sub>O or not, the activity of photocatalytic degradation of benzene by Bi/TiO<sub>2</sub> was lower than that of pure TiO<sub>2</sub> under UV irradiation. Among those investigations, the activity of Bi<sub>2</sub>O<sub>3</sub>/TiO<sub>2</sub> compound particles under solar light has not been concerned.

In this work, Bi<sub>2</sub>O<sub>3</sub>/TiO<sub>2</sub> composite particles were synthesized by sol-gel method under mild condition. The characterization of the as-prepared sample was measured by XRD, SEM, XPS, BET and DRS. The photocatalytic activity was evaluated under solar light irradiation for degradation of 4-chlorophenol.

## 2 Experimental

### 2.1 Catalyst preparation

Bi<sub>2</sub>O<sub>3</sub> powders were purchased from Sinopham Chemical Reagent Co., Ltd, with a size range of 0.5–2  $\mu$ m and mainly in monoclinic phase. Titanium (IV)-*n*-butoxide (Ti(OBu)<sub>4</sub>) was used as Ti precursor. Bi<sub>2</sub>O<sub>3</sub> was firstly added into abundant water, the pH value of which was adjusted to 2.0 by HNO<sub>3</sub>. Then the mixture of Ti(OBu)<sub>4</sub> and isopropyl alcohol was added dropwise into the solution. After complete hydrolysis of Ti(OBu)<sub>4</sub>, the solution was refluxed at 70 °C for 20 h and a sol solution formed. Finally, the as-prepared sol was vacuum dried at 60 °C for 2 h to obtain Bi<sub>2</sub>O<sub>3</sub>/TiO<sub>2</sub> composite powders. For comparison, pure TiO<sub>2</sub> powders were also synthesized using the method mentioned above without adding Bi<sub>2</sub>O<sub>3</sub>.

### 2.2 Characterization

The as-prepared samples were identified by X-ray diffractometer (XRD, XD-3A, Shimadzu Corporation, Japan) using graphite monochromatic copper radiation (Cu K <sub>$\alpha$</sub> ) at 40 kV, 30 mA over the  $2\theta$  range of 20°–80°. The morphologies were characterized with a scanning electron microscope (SEM, Sirion, FEI). BET surface area measurements were carried out by N<sub>2</sub> adsorption at 77 K using an ASAP2020 instrument. The total pore volume was calculated from the amount of nitrogen adsorbed at relative pressure of 0.975. The binding energy was identified by X-ray photoelectron spectroscopy (XPS) with Mg K <sub>$\alpha$</sub>  radiation (ESCALB-250). A UV-vis spectrophotometer (Shimadzu UV-4100) was used to record the diffuse reflectance spectra of samples.

### 2.3 Photocatalytic degradation experiments

The photocatalytic activity of Bi<sub>2</sub>O<sub>3</sub>/TiO<sub>2</sub> particles

was investigated by degradation of 4-chlorophenol in the aqueous solution. The bench-scale photoreactor system was composed of a cylindrical silica reactor, and a light filter cutting light with wavelength shorter than 400 nm providing artificial solar light from vertical irradiation. A set of photocatalytic degradation experiments were performed with the following procedure: 200 mg TiO<sub>2</sub> powder was added into 200 mL 4-chlorophenol solution of 50 mg/L. The suspension was stirred in dark for 30 min to obtain adsorption equilibrium of 4-chlorophenol before illumination. At a defined time interval, 5 mL suspension was removed and the concentration of 4-chlorophenol was analyzed using the UV-vis spectrophotometer at 280 nm.

## 3 Results and discussion

### 3.1 XRD analysis

The X-ray diffraction (XRD) patterns of Bi<sub>2</sub>O<sub>3</sub>/TiO<sub>2</sub>, pure TiO<sub>2</sub> and Bi<sub>2</sub>O<sub>3</sub> powders are shown in Fig.1. It can be seen that two crystalline phases are identified from the XRD patterns of TiO<sub>2</sub>, namely the major phase is anatase, and the minor phase is brookite. Bi<sub>2</sub>O<sub>3</sub> is mainly in monoclinic phase. As for Bi<sub>2</sub>O<sub>3</sub>/TiO<sub>2</sub>, the peak at 25.4° is broadened, indicating that there exist more than one peak, which may contain anatase and  $\alpha$ -bismuth oxide peaks compared with those of Bi<sub>2</sub>O<sub>3</sub> and pure TiO<sub>2</sub>. No new phase is detected, which indicates that the TiO<sub>2</sub> particles were only adsorbed on the surface of Bi<sub>2</sub>O<sub>3</sub>.

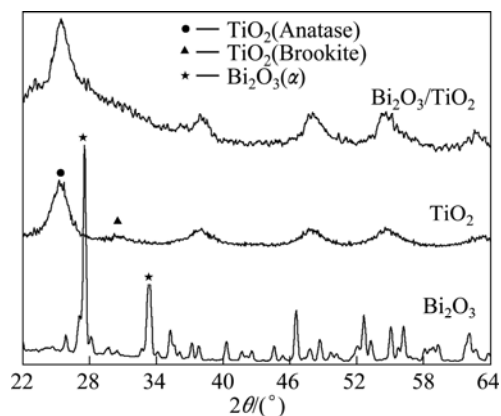
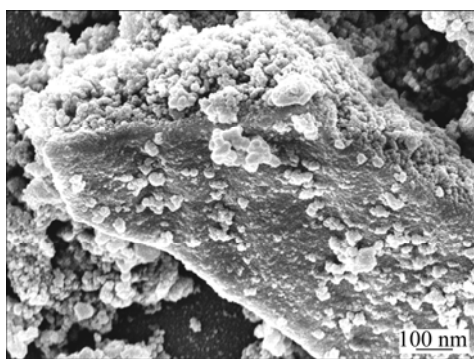


Fig.1 XRD patterns of samples

### 3.2 Microstructure

In order to probe the interaction among the components in the composite photocatalysts, these photocatalysts were investigated. The SEM image of Bi<sub>2</sub>O<sub>3</sub>/TiO<sub>2</sub> sample is shown in Fig.2. A big particle with regular monoclinic structure in micrometer size is  $\alpha$ -Bi<sub>2</sub>O<sub>3</sub>, and the clusters deposited on the surface of Bi<sub>2</sub>O<sub>3</sub> are TiO<sub>2</sub> nanoparticles. It can be seen that the composite sample is composed of micro-scale Bi<sub>2</sub>O<sub>3</sub> particles and sub-micro-scale clusters containing titania nano-particles. This micro-nano structure with

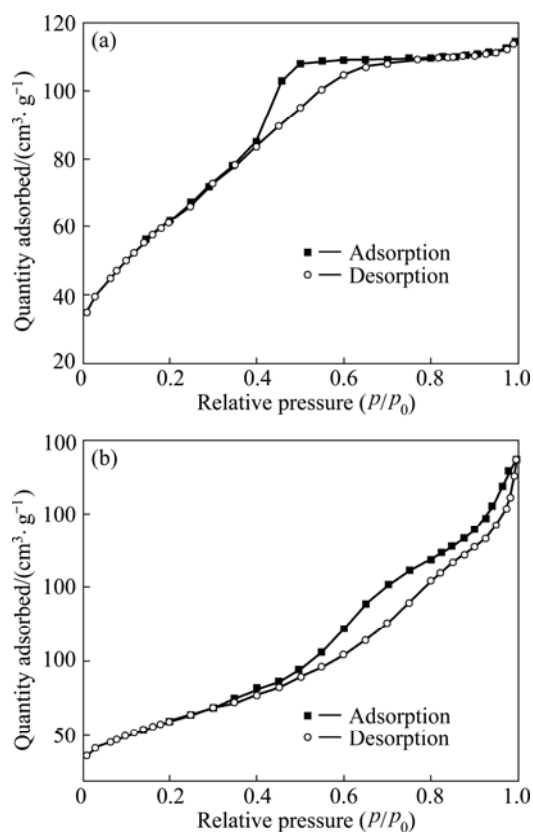


**Fig.2** SEM image of  $\text{Bi}_2\text{O}_3/\text{TiO}_2$  particles

hierarchical structure containing micro, sub-micro and nano-scale particles may be beneficial for the achievement of various photo-electric properties[18]. On the other hand, the dispersity of titania is enhanced. Therefore, this structure can offer more active adsorption sites and photocatalytic reaction centers.

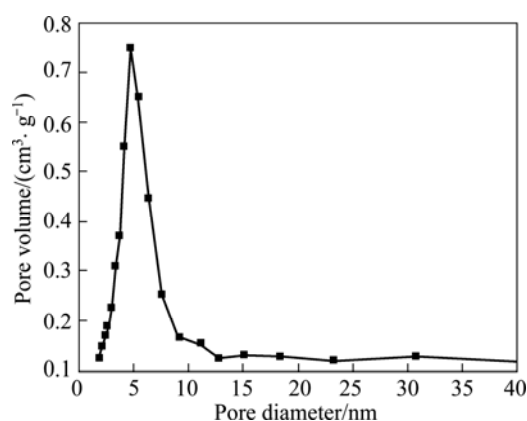
### 3.3 BET

Fig.3 shows nitrogen adsorption-desorption isotherms of  $\text{TiO}_2$  and  $\text{Bi}_2\text{O}_3/\text{TiO}_2$ . Both samples show the isotherm of type IV (BDDT classification)[19]. At high relative pressure from 0.4 to 0.8, the isotherms of  $\text{TiO}_2$  and  $\text{Bi}_2\text{O}_3/\text{TiO}_2$  exhibit hysteresis loops of type H2 and H3, respectively, this indicates that the powders contained mesopores (2–50 nm).



**Fig.3** Adsorption-desorption isotherms of  $\text{TiO}_2$  (a) and  $\text{Bi}_2\text{O}_3/\text{TiO}_2$  (b)

Fig.4 shows the pore diameter distribution of  $\text{Bi}_2\text{O}_3/\text{TiO}_2$ . It can be seen that the diameter range of pore mainly distributes from 2.0 to 9.0 nm, and the average pore diameter is 5.0 nm, which is larger than the value of 3.2 nm for  $\text{TiO}_2$ . The formation of mesoporous structure in  $\text{TiO}_2$  and  $\text{Bi}_2\text{O}_3/\text{TiO}_2$  is attributed to the aggregation of  $\text{TiO}_2$  particles[20–21]. As seen from Table 1, the BET surface area of the composite  $\text{Bi}_2\text{O}_3/\text{TiO}_2$  is smaller than that of pure titania due to the bigger nonporous particles of  $\text{Bi}_2\text{O}_3$ . When the pore volume becomes larger, bigger crystallites aggregate to bigger pores[21].



**Fig.4** Pore diameter distribution of  $\text{Bi}_2\text{O}_3/\text{TiO}_2$

**Table 1** BET data for  $\text{TiO}_2$  and  $\text{Bi}_2\text{O}_3/\text{TiO}_2$

Sample	BET surface area/( $\text{m}^2\cdot\text{g}^{-1}$ )	Pore volume/( $\text{cm}^3\cdot\text{g}^{-1}$ )	Average pore size /nm
$\text{TiO}_2$	229.2	0.17	3.2
$\text{Bi}_2\text{O}_3/\text{TiO}_2$	215.1	0.32	5.0

### 3.4 XPS

In order to analyze the chemical composition and purity of the prepared samples, the XPS spectrum of  $\text{Bi}_2\text{O}_3/\text{TiO}_2$  was measured. The high-resolution XPS spectra of Bi 4f, Ti 2p and O 1s regions on the surface of samples are shown in Fig.5. The peaks of Bi 4f 7/2 and Bi 4f 5/2 are centered at 164.2 and 158.9 eV, respectively, which are consistent with those of  $\text{Bi}^{3+}$ , as reported in Ref.[17]. This XPS spectrum demonstrates that the main valence of Bi in the prepared sample is +3 in  $\text{Bi}_2\text{O}_3$ . Ti 2p 1/2 and Ti 2p 3/2 spin-orbital splitting photoelectrons were located at the binding energies of about 464.3 and 458.2 eV, respectively. In general, large binding energy means more oxidized metal[22]. However, no evidence indicated that the band shifted to higher binding energy when  $\text{Bi}_2\text{O}_3$  was incorporated with  $\text{TiO}_2$ , which was also confirmed by KANG et al[16]. As shown in Fig. 5(c), the O 1s spectra of both  $\text{TiO}_2$  and  $\text{Bi}_2\text{O}_3/\text{TiO}_2$  samples are fitted to two peaks, respectively. The lower binding energy of 529.8 eV is attributed to Ti—O in  $\text{TiO}_2$  crystal

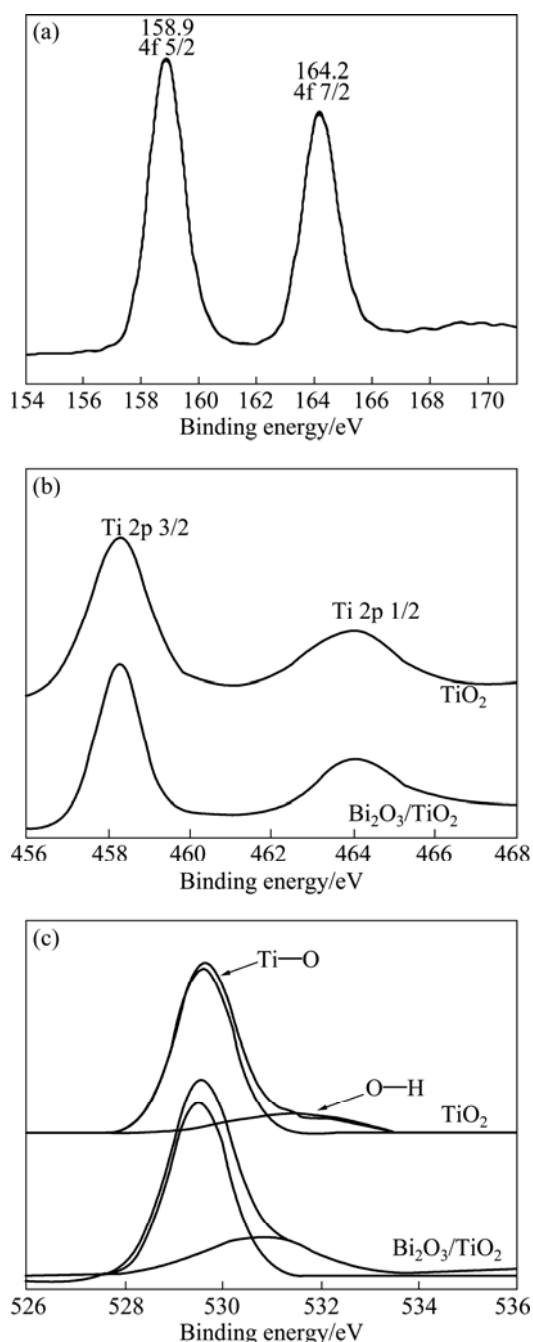


**Fig.5** XPS patterns of  $\text{Bi}_2\text{O}_3/\text{TiO}_2$  composite samples: (a) Bi 4f, (b) Ti 2p; (c) O 1s core level

lattice, and the higher binding energy of 531.4 eV is related to O—H resulting from chemisorbed water[23]. The amount ratio of O—H/Ti—O for  $\text{Bi}_2\text{O}_3/\text{TiO}_2$  increases compared with pure  $\text{TiO}_2$ . The ratios are 0.41 and 0.21, respectively. It illuminates that the number of surface hydroxyl groups of  $\text{TiO}_2$  is increased when incorporated with  $\text{Bi}_2\text{O}_3$ , and subsequently free hydroxyl radicals which was proved to be beneficial for photocatalytic reactions[24] can be also increased.

### 3.5 DRS

The UV-vis diffuse reflectance spectra of  $\text{TiO}_2$  and

$\text{Bi}_2\text{O}_3/\text{TiO}_2$  are shown in Fig.6. It can be seen that there is a significant shift in the onset absorption towards the higher wavelength of  $\text{Bi}_2\text{O}_3/\text{TiO}_2$ . As known from XRD pattern, no new phase appears in  $\text{Bi}_2\text{O}_3/\text{TiO}_2$ , indicating that it is not  $\text{Bi}_{12}\text{Ti}_{20}$  with band gap of 2.4 eV[25] or other phase leads to red shift, but the band gap of  $\alpha\text{-Bi}_2\text{O}_3$  of 2.85 eV responds to visible irradiation.

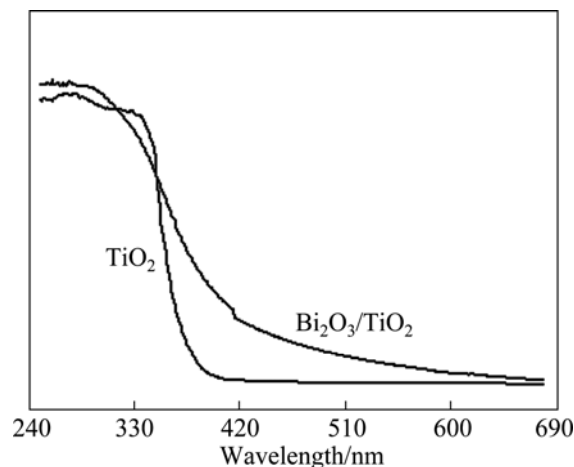


**Fig.6** UV-vis diffuse reflectance spectra of  $\text{TiO}_2$  and  $\text{Bi}_2\text{O}_3/\text{TiO}_2$

### 3.6 Photocatalytic activity

The photocatalytic activity of  $\text{TiO}_2$  and  $\text{Bi}_2\text{O}_3/\text{TiO}_2$  particles were studied by decomposition of 4-chlorophenol aqueous solution under solar light illumination. It can be seen from Fig.7 that  $\text{Bi}_2\text{O}_3/\text{TiO}_2$  exhibits much higher photocatalytic activity than  $\text{TiO}_2$  or P25. The degradation rates of  $\text{Bi}_2\text{O}_3/\text{TiO}_2$ ,  $\text{TiO}_2$  and P25 are 78.6%, 20.8% and 6.1%, respectively, which is in good agreement with analyses forenamed. It is well known that the photocatalytic oxidation of organic pollutants in aqueous suspension follows Langmuir-Hinshelwood model:

$$-dc/dt = k_r K_a c / (1 + K_a c) \quad (1)$$

where  $(-dc/dt)$  is the degradation rate of 4-chlorophenol;  $c$  is the 4-chlorophenol concentration in the solution;  $t$  is reaction time;  $k_r$  is the reaction rate constant; and  $K_a$  is the adsorption coefficient of the reactant.  $K_a c$  is negligible when the value of  $c$  is very small. As a result, Eq.(1) can be described as a first-order kinetics. Set Eq.(1) under the initial conditions of the photocatalytic procedure, when  $t=0$ ,  $c=c_0$ , it can be described as

$$\ln(c_0 / c) = k_{app} t \quad (2)$$

where  $k_{app}$  is the apparent rate constant, used as the basic kinetic parameter for different photocatalysts, and it can determine the photocatalytic activity independent of the previous adsorption period in the dark and the concentration of 4-chlorophenol remaining in the

solution[26]. The variations in  $\ln(c_0/c)$  as a function of irradiation time are given in Fig.8, and the corresponding  $k_{app}$  and  $R$  (regression relative coefficient) are given in Table 2, which confirms that  $k_{app}$  is enhanced by incorporating  $\text{TiO}_2$  with  $\text{Bi}_2\text{O}_3$ , under solar illumination compared with pure one.

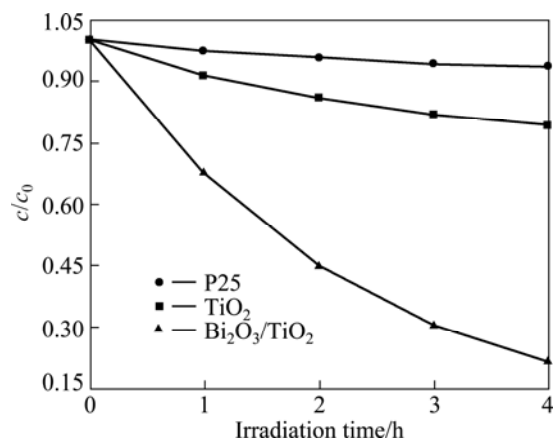


**Fig.7** Kinetic of 4-chlorophenol degradation with different samples

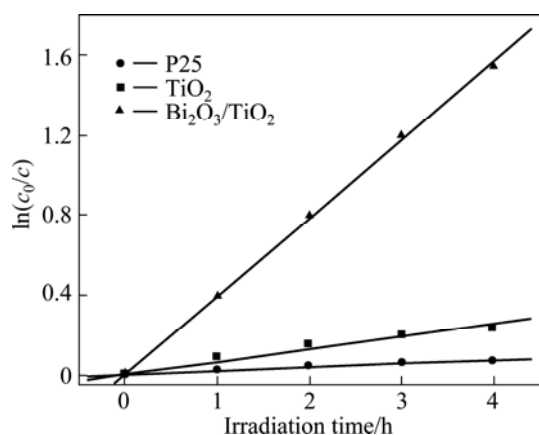


**Fig.8** Variations in  $\ln(c_0/c)$  as function of irradiation time and linear fits of samples

**Table 2**  $k_{app}$  and  $R$  data for each sample

Sample	Light source	$k_{app}/\text{h}^{-1}$	$R$
P25	Solar	0.016	0.981
TiO <sub>2</sub>	Solar	0.058	0.982
Bi <sub>2</sub> O <sub>3</sub> /TiO <sub>2</sub>	Solar	0.392	0.998

## 4 Conclusions

1) The as-prepared material does not form new crystal phase besides anatase from  $\text{TiO}_2$  and monoclinic  $\text{Bi}_2\text{O}_3$  phase. Depositing  $\text{TiO}_2$  nanoparticles on  $\text{Bi}_2\text{O}_3$  surface can form micro-nano structure.

2)  $\text{Bi}_2\text{O}_3/\text{TiO}_2$  composite particles exhibit porosity and increased surface hydroxyl groups. Furthermore, more active adsorption sites and photocatalytic reaction centers can be offered due to their special structure.

3) Owing to the narrow band gap of  $\alpha\text{-Bi}_2\text{O}_3$ ,  $\text{Bi}_2\text{O}_3/\text{TiO}_2$  shows red shift compared with pure  $\text{TiO}_2$ . The photocatalytic activity of  $\text{Bi}_2\text{O}_3/\text{TiO}_2$  has been enhanced a lot compared with P25 and pure  $\text{TiO}_2$  under sunlight.

## References

- [1] HOFFMANN M R, MARTIN S T, CHOI W, BAHNEMANN D W. Environmental applications of semiconductor photocatalysis [J]. Chem Rev, 1995, 95(1): 69–96.
- [2] WANG Chao, AO Yan-hui, WANG Pei-fang, HOU Jun, QIAN Jin, ZHANG Song-he. Preparation, characterization, photocatalytic properties of titania hollow sphere doped with cerium [J]. J Hazard Mater, 2010, 178(1–3): 517–521.
- [3] WANG Chao, AO Yan-hui, WANG Pei-fang, HOU Jun, QIAN Jin. Photocatalytic performance of Gd ion modified titania porous hollow spheres under visible light [J]. Mater Letts, 2010, 64(8): 1003–1006.
- [4] ARAI Y, TANAKA K, KHLAIFAT A L. Photocatalysis of  $\text{SiO}_2$ -loaded  $\text{TiO}_2$  [J]. J Mole Catal A, 2006, 243(1): 85–88.
- [5] BISWAS S, HOSSAIN M F, TAKAHASHI T, KUBOTA Y, FUJISHIMA A. Photocatalytic activity of high-vacuum annealed  $\text{CdS-TiO}_2$  thin film [J]. Thin Solid Film, 2008, 516(21): 7313–7317.
- [6] HOUŠKOVÁ V, ŠTENGL V, BAKARDJIEVA S, MURAF A N. Photoactive materials prepared by homogeneous hydrolysis with thioacetamide: Part 2— $\text{TiO}_2/\text{ZnO}$  nanocomposites [J]. J Phys Chem Solid, 2008, 69(7): 1623–1631.
- [7] LEE H C, HWANG W S. Substrate effects on the oxygen gas sensing properties of  $\text{SnO}_2/\text{TiO}_2$  thin films [J]. Appl Surf Sci, 2006, 253(4): 1889–1897.
- [8] SERPONE N, PICHAT P, PILIZZETTI E, HIDAKA H. Exploiting the interparticle electron transfer process in the photocatalysed oxidation of phenol, 2-chlorophenol and pentachlorophenol: chemical evidence for electron and hole transfer between coupled semiconductors [J]. J Photochem Photobiol A, 1995, 85(3): 247–255.
- [9] SHINGUU H, BHUIYAN M M H, IKEGAMI T, EBIHARA K. Preparation of  $\text{TiO}_2/\text{WO}_3$  multilayer thin film by PLD method and its catalytic response to visible light [J]. Thin Solid Films, 2006, 506–507: 111–114.
- [10] LEONTIE L, CARAMAN M, ALEXE M, HARNAGEA C. Structural and optical characteristics of bismuth oxide thin films [J]. Surf Sci, 2002, 507–510: 480–485.
- [11] TOMCHENKO A A. Structure and gas-sensitive properties of  $\text{WO}_3\text{-Bi}_2\text{O}_3$  mixed thick Films [J]. Sensor Actuat B, 2000, 68(1–3): 48–52.
- [12] SHIMIZUGAWA K, SUGIMOTO M, MIURA N, YAMAZOE N. Bismuth oxide thin film as new electrochromic material [J]. Solid State Ionics, 1998, 113–115: 415–419.
- [13] MONNEREAU O, TORTET L, LLEWELLYN P, ROUQUEROL F, VACQUIER G. Synthesis of  $\text{Bi}_2\text{O}_3$  by controlled transformation rate thermal analysis: A new route for this oxide [J]. Solid State Ionics, 2003, 157(1–4): 163–169.
- [14] GUALTIERI A F, IMMOVILLI S, PRUDENZIATI M. Reduction process of  $\text{RuO}_2$  powder and kinetics of compound omega- $\text{Bi}_2\text{O}_3$  [J]. Powder Diffract, 1997, 12(2): 90–92.
- [15] DOLOCAN V. Transmission spectra of bismuth trioxide thin films [J]. Appl Phys, 1978, 16: 405–407.

- [16] KANG M, KO Y R, JEON M K, LEE S C, CHOUNG S J, PARK J Y, KIM S, CHOI S H. Characterization of Bi/TiO<sub>2</sub> nanometer sized particle synthesized by solvothermal method and CH<sub>3</sub>CHO decomposition in a plasma-photocatalytic system [J]. J Photochem Photobio A, 2005, 173(2): 128–136.
- [17] HONG W J, KANG M. The super-hydrophilicities of Bi-TiO<sub>2</sub>, V-TiO<sub>2</sub>, and Bi-V-TiO<sub>2</sub> nano-sized particles and their benzene photodecompositions with H<sub>2</sub>O addition [J]. Mater Lett, 2006, 60(9–10): 1296–1305.
- [18] ZHAO Yao, ZHAI Jin, TAN Shu-xin, WANG Li-fang, JIANG Lei, ZHU Dao-ben. TiO<sub>2</sub> micro/nano-composite structured electrodes for quasi-solid-state dye-sensitized solar cells [J]. Nanotechnol, 2006, 17(9): 2090–2097.
- [19] SING K S W, EVERETT D H, HAUL R A W, MOSCOU L, PIEROTTI R A, ROUQUEROL J, SIEMIENIEWSKA T. Reporting physisorption data for gas/solid systems with special reference to the determination of surface area and porosity [J]. Pure Appl Chem, 1985, 57(4): 603–619.
- [20] AO Yan-hui, XU Jing-jing, FU De-gang. Deposition of anatase titania onto carbon encapsulated magnetite nanoparticles [J]. Nanotechnol, 2008, 19: 405604.
- [21] YU Jia-guo, ZHOU Ming-hua, CHENG Bei, YU Huo-gen, ZHAO Xiu-jian. Ultrasonic preparation of mesoporous titanium dioxide nanocrystalline photocatalysts and evaluation of photocatalytic activity [J]. J Mole Catal A, 2005, 227(1–2): 75–80.
- [22] XIN J H, ZHANG S M, QI G D, ZHENG X C, HUANG W P, WU S H. Preparation and characterization of the Bi-doped TiO<sub>2</sub> photocatalysts [J]. React Kinet Catal Lett, 2005, 86(2): 291–298.
- [23] JING Li-qiang, XIN Bai-fu, YUAN Fu-long, XUE Lian-peng, WANG Bai-qi, FU Hong-gang. Effects of surface oxygen vacancies on photophysical and photochemical processes of Zn-doped TiO<sub>2</sub> nanoparticles and their relationships [J]. J Phys Chem B, 2006, 110(36): 17860–17865.
- [24] MROWETZ M, SELLI E. H<sub>2</sub>O<sub>2</sub> evolution during the photocatalytic degradation of organic molecules on fluorinated TiO<sub>2</sub> [J]. New J Chem, 2006, 30(1): 108–114.
- [25] YAO W F, WANG H, XU X H, CHENG X F, HUANG J, SHANG S X, YANG X N, WAN G M. Photocatalytic property of bismuth titanate Bi<sub>12</sub>TiO<sub>20</sub> crystals [J]. Appl Catal A, 2003, 243(1): 185–190.
- [26] MATOS J, LAINE J, HERRMANN J M. Synergy effect in the photocatalytic degradation of phenol on a suspended mixture of titania and activated carbon [J]. Appl Catal B, 1998, 18(3–4): 281–291.

## 氧化铋/二氧化钛复合颗粒的制备及其光催化降解 4-氯苯酚的性能

徐晶晶<sup>1,2</sup>, 陈敏东<sup>1</sup>, 付德刚<sup>3</sup>

1. 南京信息工程大学 环境科学与工程学院 江苏省大气环境监测与污染控制高技术研究重点实验室, 南京 210044;
2. 河海大学 水文水资源与水利工程科学国家重点实验室, 南京 210098;
3. 东南大学 生物电子学国家重点实验室, 南京 210096

**摘要:** 在低温条件下制备在太阳光照射下具有高光催化活性的氧化铋/二氧化钛复合颗粒。并利用 XRD、SEM、BET、XPS 和 DRS 对其进行表征。结果表明: 将二氧化钛纳米颗粒沉积在氧化铋表面可形成微-纳结构, 使该复合材料表现出多孔性, 并提高表面羟基的含量。因此, 在太阳光的激发下, 氧化铋/二氧化钛复合颗粒对 4-氯苯酚的催化降解能力高于纯二氧化钛和 P25。

**关键词:** 氧化铋; 二氧化钛; 光催化; 4-氯苯酚

(Edited by FANG Jing-hua)